Available online at www.sciencedirect.com
ScienceDirect
Journal of Sound and Vibration 310 (2008) 217–229
JOURNAL OF SOUND AND VIBRATION
www.elsevier.com/locate/jsvi

A new explicit predictor–multicorrector high-order accurate method for linear elastodynamics

A.V. Idesman[a,*], M. Schmidt[b], R.L. Sierakowski[b]

[a]*Department of Mechanical Engineering, Texas Tech University, Lubbock, TX 79409-1021, USA*
[b]*Air Force Research Laboratory, Munitions Directorate, Eglin Air Force Base, FL 32542, USA*

Received 1 February 2007; received in revised form 27 July 2007; accepted 30 July 2007
Available online 21 September 2007

Abstract

A new explicit predictor–multicorrector high-order accurate method is suggested for linear elastodynamics. The method is derived from the implicit high-order accurate method based on the time-continuous Galerkin method proposed earlier in our papers. The basic unknowns for the method are displacements and velocities; accelerations are not calculated. The explicit method uses a predictor–multicorrector technique with one or two passes in order to reach the fourth order of accuracy and has controllable numerical dissipation for the suppression of spurious high-frequency oscillations. In contrast to recently suggested explicit high-order accurate methods based on the time-discontinuous Galerkin method, the new method is more accurate (has a higher order of accuracy) and has better algorithmic properties (e.g., a higher-stability limit) at the same computational efforts. Presented numerical examples show the performance of the new method. The method appears to be competitive for medium- and long-term analysis when accuracy of numerical solutions arises an issue due to error accumulation.

1. Introduction

Most finite-element procedures for elastodynamics problems are based upon semi-discrete methods (see Refs. [1–3] and others) and have the second order of accuracy. Zienkiewich and coworkers (see Refs. [3–5]) have developed and analyzed a set of algorithms, called the unified set of a single-step method, based on the application of the weighted residual method to the equation of motion. Many of the classical finite-difference schemes are particular cases of the unified set. High accuracy in time can be obtained by using higher-order interpolation polynomials. Recently, new high-order accurate methods with a step-by-step time integration scheme have been developed for elastodynamics (see Refs. [6–11] and others). Most of them are based on semi-discrete equations with the polynomial time approximations of unknown functions. The polynomial coefficients are derived with the use of different approaches such as the time-continuous Galerkin (TCG) and time-discontinuous Galerkin (TDG) methods, weighted residual methods, collocation methods and others.

*Corresponding author.
E-mail address: alexander.idesman@coe.ttu.edu (A.V. Idesman).

0022-460X/$ - see front matter © 2007 Elsevier Ltd. All rights reserved.
doi:10.1016/j.jsv.2007.07.052

The aforementioned methods for elastodynamics use implicit or explicit time integration schemes. Implicit methods include the solution of a system of algebraic equations, are usually unconditionally stable and allow large time increments. Explicit methods are implemented with a diagonal mass matrix and do not require the solution of a system of algebraic equations, but are only conditionally stable (i.e., time increments have to be smaller than the stability limit). Wave propagation problems usually require small time increments, therefore explicit methods are often used for these kinds of problems. The second-order central difference method is still the most popular explicit method. In our study, we will develop a new fourth-order accurate explicit method for linear elastodynamics. This method will be derived from the high-order accurate implicit TCG method suggested recently in our papers [12,13] (the new implicit method is much faster than known implicit methods for linear elastodynamics at the same accuracy). The explicit method is based on a predictor–multicorrector technique with one or two passes and has controllable numerical dissipation for the suppression of spurious oscillations. It is interesting to note that the new explicit method has numerical dissipation even when derived from a non-dissipative implicit TCG method. The basic unknowns for the method are displacements and velocities; accelerations are not calculated. In contrast to the known explicit high-order accurate methods for elastodynamics that are based on the TDG method (see Refs. [6,11]), the new method is more accurate (has a higher order of accuracy) and has better algorithmic properties (e.g., a higher-stability limit) at the same computational efforts.

The paper is organized as follows. First, we will describe the new implicit high-order accurate method proposed in Refs. [12,13], which is based on the TCG method. Then we will derive from this method a new explicit 4th-order accurate method. Next, accuracy analysis of the new method will be presented showing advantages of the new method in comparison with the known explicit high-order accurate methods for elastodynamics based on the TDG method (see Refs. [6,11]). Finally, numerical examples showing the performance of the new method will be considered.

2. Weak and discrete formulations of elastodynamics based on the continuous Galerkin time-stepping method

For the derivation of weak and discrete formulations of elastodynamics, the so-called two-field formulation is used. For this aim the finite-element equations can be rewritten as follows:

$$\mathbf{M}\dot{\mathbf{V}} + \mathbf{C}\mathbf{V} + \mathbf{K}\mathbf{U} = \mathbf{R}, \quad \mathbf{V} = \dot{\mathbf{U}}, \tag{1}$$

where $\mathbf{M}$, $\mathbf{C}$, $\mathbf{K}$ are the mass, damping and stiffness matrices, respectively, $\mathbf{U}(t)$ is the vector of the nodal displacement, $\mathbf{V}(t)$ is the vector of the nodal velocity, and $\mathbf{R}(t)$ is the vector of the nodal load. Eqs. (1) are a system of ordinary differential equations. For the continuous Galerkin time-stepping method, we introduce a partition of the whole time interval $[0, T]$ in a not necessarily uniform fashion by $0 = t_0 < t_1 < \cdots < t_n < \cdots < t_N$ and define the time intervals $J_n = [t_{n-1}, t_n]$, $n = 1, \ldots, N$, where $t_N = T$. A weak formulation of elastodynamics for any time interval J_n can be derived from Eqs. (1) as follows:

$$\int_{J_n} (\bar{\mathbf{v}}^{\mathrm{T}} + a\dot{\bar{\mathbf{v}}}^{\mathrm{T}})[\mathbf{M}\dot{\mathbf{V}} + \mathbf{C}\mathbf{V} + \mathbf{K}\mathbf{U} - \mathbf{R}]\lambda_1(t)\,\mathrm{d}t = 0, \tag{2}$$

$$\int_{J_n} (\bar{\mathbf{u}}^{\mathrm{T}} + a\dot{\bar{\mathbf{u}}}^{\mathrm{T}})(\dot{\mathbf{U}} - \mathbf{V})\lambda_2(t)\,\mathrm{d}t = 0, \tag{3}$$

where $\bar{\mathbf{u}}(t)$ and $\bar{\mathbf{v}}(t)$ are the test vector functions depending on time t; a is the scalar coefficient and has the dimension of time (e.g., s); $\lambda_1(t)$ and $\lambda_2(t)$ are the weighting scalar functions depending on time t only. At time t_{n-1} nodal displacements and velocities $\mathbf{U}(t_{n-1})$ and $\mathbf{V}(t_{n-1})$ are known from the solution for the previous time interval J_{n-1}, or from the initial conditions, and $\bar{\mathbf{u}}(t_{n-1}) = \bar{\mathbf{v}}(t_{n-1}) = \mathbf{0}$. For any time interval, J_n a local time $t^* = t - t_{n-1}$ can be introduced. Time t^* varies from 0 to Δt ($\Delta t = t_n - t_{n-1}$). For convenience, for all derivations for time intervals J_n, the local time t^* will be used. However, in order to simplify notations, the local time will be designated as t. The advantages of using additional scalar functions $\lambda_1(t)$ and $\lambda_2(t)$ were considered in our paper [13]. At special polynomial approximations of these functions, they do not affect the order of accuracy of the numerical algorithm but allow control of additional algorithmic characteristics;

e.g., the spectral radii [13]. For simplicity the case with $\lambda_1(t)=\lambda_2(t)=1$ is considered. The numerical algorithm with polynomial functions $\lambda_1(t)$ and $\lambda_2(t)$ can be derived without any difficulties.

To get a discrete formulation from Eqs. (2) and (3) the following time polynomial approximations of the order n for any time interval J_n will be used for $\mathbf{U}(t)$, $\mathbf{V}(t)$, $\bar{\mathbf{u}}(t)$ and $\bar{\mathbf{v}}(t)$:

$$\mathbf{U}(t)=\mathbf{U}_0+\mathbf{U}_1 t+\mathbf{U}_2 t^2+\cdots+\mathbf{U}_n t^n, \tag{4}$$

$$\mathbf{V}(t)=\mathbf{V}_0+\mathbf{V}_1 t+\mathbf{V}_2 t^2+\cdots+\mathbf{V}_n t^n, \tag{5}$$

$$\bar{\mathbf{u}}(t)=\bar{\mathbf{u}}_0+\bar{\mathbf{u}}_1 t+\bar{\mathbf{u}}_2 t^2+\cdots+\bar{\mathbf{u}}_n t^n, \tag{6}$$

$$\bar{\mathbf{v}}(t)=\bar{\mathbf{v}}_0+\bar{\mathbf{v}}_1 t+\bar{\mathbf{v}}_2 t^2+\cdots+\bar{\mathbf{v}}_n t^n, \tag{7}$$

where $\mathbf{U}_0$ and $\mathbf{V}_0$ are the known initial displacement and velocity, $\mathbf{U}_1,\ldots,\mathbf{U}_n$ and $\mathbf{V}_1,\ldots,\mathbf{V}_n$ are unknown vectors to be determined, $\bar{\mathbf{u}}_0=\bar{\mathbf{v}}_0=\mathbf{0}$, and $\bar{\mathbf{u}}_1,\ldots,\bar{\mathbf{u}}_n$ and $\bar{\mathbf{v}}_1,\ldots,\bar{\mathbf{v}}_n$ are test vectors. When Eqs. (4)–(7) are inserted into Eqs. (2) and (3), the final discrete system of algebraic equations for unknowns $\mathbf{U}_1,\ldots,\mathbf{U}_n$ and $\mathbf{V}_1,\ldots,\mathbf{V}_n$ is derived as follows:

$$\begin{aligned}&(\mathbf{M}\mathbf{V}_1+\mathbf{C}\mathbf{V}_0+\mathbf{K}\mathbf{U}_0)\left(\frac{\Delta t}{1+k}+a\right)+(2\mathbf{M}\mathbf{V}_2+\mathbf{C}\mathbf{V}_1+\mathbf{K}\mathbf{U}_1)\left(\frac{\Delta t}{2+k}+\frac{ak}{k+1}\right)\Delta t\\&+\cdots+(n\mathbf{M}\mathbf{V}_n+\mathbf{C}\mathbf{V}_{n-1}+\mathbf{K}\mathbf{U}_{n-1})\left(\frac{\Delta t}{n+k}+\frac{ak}{n+k-1}\right)\Delta t^{n-1}\\&+(\mathbf{C}\mathbf{V}_n+\mathbf{K}\mathbf{U}_n)\left(\frac{\Delta t}{n+k+1}+\frac{ak}{n+k}\right)\Delta t^n=\mathbf{R}_k,\quad k=1,2,\ldots,n\end{aligned} \tag{8}$$

$$\begin{aligned}&(\mathbf{U}_1-\mathbf{V}_0)\left(\frac{\Delta t}{1+k}+a\right)+(2\mathbf{U}_2-\mathbf{V}_1)\left(\frac{\Delta t}{2+k}+\frac{ak}{k+1}\right)\Delta t+\cdots+(n\mathbf{U}_n-\mathbf{V}_{n-1})\left(\frac{\Delta t}{n+k}+\frac{ak}{n+k-1}\right)\Delta t^{n-1}\\&-\mathbf{V}_n\left(\frac{\Delta t}{n+k+1}+\frac{ak}{n+k}\right)\Delta t^n=\mathbf{0},\quad k=1,2,\ldots,n,\end{aligned} \tag{9}$$

where

$$\mathbf{R}_k=\frac{1}{\Delta t^k}\int_0^{\Delta t}\mathbf{R}(t)(t^k+akt^{k-1})\,\mathrm{d}t. \tag{10}$$

This procedure can be considered as the application of the continuous Galerkin method to the system (1). Eqs. (8) and (9) represent a system of $2n$ algebraic equations with $2n$ unknown vectors $\mathbf{U}_1,\ldots,\mathbf{U}_n$ and $\mathbf{V}_1,\ldots,\mathbf{V}_n$. It is necessary to note that the system of n equations (9) can be analytically solved separately from the system (8); i.e., unknown vectors $\mathbf{V}_1,\ldots,\mathbf{V}_n$ can be expressed in terms of unknown vectors $\mathbf{U}_1,\ldots,\mathbf{U}_n$. Then the final system of Eqs. (8) and (9) can be reduced to a system of only n equations with unknown vectors $\mathbf{U}_1,\ldots,\mathbf{U}_n$. Let us consider the derivation of the final system of equations for $n=2$ in detail, see also our paper [12]. For higher values of n the derivation is similar to this case.

3. A new fourth-order accurate implicit method

For the quadratic approximations of vectors $\mathbf{U}(t)$, $\mathbf{V}(t)$, $\bar{\mathbf{u}}(t)$ and $\bar{\mathbf{v}}(t)$, Eqs. (4)–(7) can be rewritten as follows:

$$\begin{aligned}&\mathbf{U}(t)=\mathbf{U}_0+\mathbf{U}_1 t+\mathbf{U}_2 t^2,\quad \mathbf{V}(t)=\mathbf{V}_0+\mathbf{V}_1 t+\mathbf{V}_2 t^2,\\&\bar{\mathbf{u}}(t)=\bar{\mathbf{u}}_0+\bar{\mathbf{u}}_1 t+\bar{\mathbf{u}}_2 t^2,\quad \bar{\mathbf{v}}(t)=\bar{\mathbf{v}}_0+\bar{\mathbf{v}}_1 t+\bar{\mathbf{v}}_2 t^2.\end{aligned} \tag{11}$$

Then from Eq. (9) ($n=2$, $k=1,2$) we get

$$(\mathbf{U}_1-\mathbf{V}_0)\left(\frac{\Delta t}{2}+a\right)+(2\mathbf{U}_2-\mathbf{V}_1)\left(\frac{\Delta t}{3}+\frac{a}{2}\right)\Delta t-\mathbf{V}_2\left(\frac{\Delta t}{4}+\frac{a}{3}\right)\Delta t^2=\mathbf{0}, \tag{12}$$

$$(\mathbf{U}_1-\mathbf{V}_0)\left(\frac{\Delta t}{3}+a\right)+(2\mathbf{U}_2-\mathbf{V}_1)\left(\frac{\Delta t}{4}+\frac{2a}{3}\right)\Delta t-\mathbf{V}_2\left(\frac{\Delta t}{5}+\frac{a}{2}\right)\Delta t^2=\mathbf{0}. \tag{13}$$

Solving Eqs. (12) and (13) we get

$$\mathbf{V}_1=2\mathbf{U}_2+a_1\mathbf{U}_1-a_1\mathbf{V}_0, \tag{14}$$

$$\mathbf{V}_2=a_2\mathbf{U}_1-a_2\mathbf{V}_0, \tag{15}$$

where

$$a_1=\frac{2(60a^2+32a\Delta t+6\Delta t^2)}{\Delta t(20a^2+12a\Delta t+3\Delta t^2)},\quad a_2=-\frac{10(12a^2+6a\Delta t+\Delta t^2)}{\Delta t^2(20a^2+12a\Delta t+3\Delta t^2)}. \tag{16}$$

At $n=2$ and $k=1,2$, Eq. (8) reduces to the following two equations:

$$(\mathbf{MV}_1+\mathbf{CV}_0+\mathbf{KU}_0)\frac{\Delta t+2a}{2}+(2\mathbf{MV}_2+\mathbf{CV}_1+\mathbf{KU}_1)\frac{2\Delta t+3a}{6}\Delta t +(\mathbf{CV}_2+\mathbf{KU}_2)\frac{3\Delta t+4a}{12}\Delta t^2=\mathbf{R}_1, \tag{17}$$

$$(\mathbf{MV}_1+\mathbf{CV}_0+\mathbf{KU}_0)\frac{2\Delta t+6a}{6}+(2\mathbf{MV}_2+\mathbf{CV}_1+\mathbf{KU}_1)\frac{3\Delta t+8a}{12}\Delta t +(\mathbf{CV}_2+\mathbf{KU}_2)\frac{4\Delta t+10a}{20}\Delta t^2=\mathbf{R}_2. \tag{18}$$

With the insertion of Eqs. (14) and (15) into Eqs. (17) and (18), the following system can be obtained (a matrix form will be used):

$$\mathbf{B}\begin{Bmatrix}\mathbf{MU}_1\\ \mathbf{MU}_2\end{Bmatrix}+\mathbf{D}\begin{Bmatrix}\mathbf{CU}_1\\ \mathbf{CU}_2\\ \mathbf{KU}_1\\ \mathbf{KU}_2\end{Bmatrix}=\mathbf{F}\begin{Bmatrix}\mathbf{MU}_0\\ \mathbf{MV}_0\\ \mathbf{CU}_0\\ \mathbf{CV}_0\\ \mathbf{KU}_0\\ \mathbf{KV}_0\end{Bmatrix}+\begin{Bmatrix}\mathbf{R}_1\\ \mathbf{R}_2\end{Bmatrix}, \tag{19}$$

where

$$\mathbf{B}=\begin{bmatrix}b_{11}\mathbf{I} & b_{12}\mathbf{I}\\ b_{21}\mathbf{I} & b_{22}\mathbf{I}\end{bmatrix},\quad \mathbf{D}=\begin{bmatrix}d_{11}\mathbf{I} & d_{12}\mathbf{I} & d_{13}\mathbf{I} & d_{14}\mathbf{I}\\ d_{21}\mathbf{I} & d_{22}\mathbf{I} & d_{23}\mathbf{I} & d_{24}\mathbf{I}\end{bmatrix},$$

$$\mathbf{F}=\begin{bmatrix}f_{11}\mathbf{I} & f_{12}\mathbf{I} & f_{13}\mathbf{I} & f_{14}\mathbf{I} & f_{15}\mathbf{I} & f_{16}\mathbf{I}\\ f_{21}\mathbf{I} & f_{22}\mathbf{I} & f_{23}\mathbf{I} & f_{24}\mathbf{I} & f_{25}\mathbf{I} & f_{26}\mathbf{I}\end{bmatrix},$$

$$\mathbf{R}_1=\frac{1}{\Delta t}\int_0^{\Delta t}\mathbf{R}(t)(t+a)\,\mathrm{d}t,\quad \mathbf{R}_2=\frac{1}{\Delta t^2}\int_0^{\Delta t}\mathbf{R}(t)(t^2+2at)\,\mathrm{d}t. \tag{20}$$

Here $\mathbf{I}$ is the unit matrix of the order m (m is the number of nodal displacements in Eq. (1)). The coefficients b_{ij}, d_{ij} and f_{ij} can be expressed in terms of a and Δt, and are given in the matrix form as follows:

$$\begin{bmatrix}b_{11} & b_{12}\\ b_{21} & b_{22}\end{bmatrix}=\begin{bmatrix}-\dfrac{2(24a^2+9a\Delta t+\Delta t^2)}{3(20a^2+12a\Delta t+3\Delta t^2)} & 2a+\Delta t\\ -\dfrac{(40a^3+36a^2\Delta t+10a\Delta t^2+\Delta t^3)}{\Delta t(20a^2+12a\Delta t+3\Delta t^2)} & \dfrac{2(3a+\Delta t)}{3}\end{bmatrix}, \tag{21}$$

$$\begin{bmatrix} d_{11} & d_{12} & d_{13} & d_{14} \\ d_{21} & d_{22} & d_{23} & d_{24} \end{bmatrix} = \begin{bmatrix} a+\dfrac{\Delta t}{2} & \dfrac{1}{3}\Delta t(3a+2\Delta t) & \dfrac{1}{6}\Delta t(3a+2\Delta t) & \dfrac{1}{12}\Delta t^2(4a+3\Delta t) \\ a+\dfrac{\Delta t}{3} & \dfrac{1}{6}\Delta t(8a+3\Delta t) & \dfrac{1}{12}\Delta t(8a+3\Delta t) & \dfrac{1}{10}\Delta t^2(5a+2\Delta t) \end{bmatrix}, \tag{22}$$

$$\begin{bmatrix} f_{11} & f_{12} & f_{13} & f_{14} & f_{15} & f_{16} \\ f_{21} & f_{22} & f_{23} & f_{24} & f_{25} & f_{26} \end{bmatrix} = \begin{bmatrix} 0 & \dfrac{2(24a^2+9a\Delta t+\Delta t^2)}{3(20a^2+12a\Delta t+3\Delta t^2)} & 0 & 0 & a+\dfrac{\Delta t}{2} & 0 \\ 0 & \dfrac{40a^3+36a^2\Delta t+10a\Delta t^2+\Delta t^3}{\Delta t(20a^2+12a\Delta t+3\Delta t^2)} & 0 & 0 & a+\dfrac{\Delta t}{3} & 0 \end{bmatrix}. \tag{23}$$

The vectors $\mathbf{U}_1$ and $\mathbf{U}_2$ can be calculated from Eq. (19) by means of a direct solver. Then the vectors $\mathbf{V}_1$ and $\mathbf{V}_2$ can be calculated from Eqs. (14) and (15). It is necessary to note that the dimension of system (19) is twice the dimension of the system of standard methods of the second order of accuracy.

4. A new fourth-order accurate explicit method

System (19) corresponds to a new fourth-order accurate implicit method, see Ref. [12]. In order to develop a new fourth-order accurate explicit method, let us modify system (19). Let us multiply both sides of Eq. (19) by $\mathbf{B}^{-1}$. Then it follows that

$$\begin{Bmatrix} \mathbf{MU}_1 \\ \mathbf{MU}_2 \end{Bmatrix} + \mathbf{B}^{-1}\mathbf{D}\begin{Bmatrix} \mathbf{CU}_1 \\ \mathbf{CU}_2 \\ \mathbf{KU}_1 \\ \mathbf{KU}_2 \end{Bmatrix} = \mathbf{B}^{-1}\mathbf{F}\begin{Bmatrix} \mathbf{MU}_0 \\ \mathbf{MV}_0 \\ \mathbf{CU}_0 \\ \mathbf{CV}_0 \\ \mathbf{KU}_0 \\ \mathbf{KV}_0 \end{Bmatrix} + \mathbf{B}^{-1}\begin{Bmatrix} \mathbf{R}_1 \\ \mathbf{R}_2 \end{Bmatrix} \tag{24}$$

or

$$\mathbf{MU}_1 + \bar{b}_{1m}d_{m1}\mathbf{CU}_1 + \bar{b}_{1m}d_{m2}\mathbf{CU}_2 + \bar{b}_{1m}d_{m3}\mathbf{KU}_1 + \bar{b}_{1m}d_{m4}\mathbf{KU}_2 = \bar{\mathbf{R}}_1 \tag{25}$$

and

$$\mathbf{MU}_2 + \bar{b}_{2m}d_{m1}\mathbf{CU}_1 + \bar{b}_{2m}d_{m2}\mathbf{CU}_2 + \bar{b}_{2m}d_{m3}\mathbf{KU}_1 + \bar{b}_{2m}d_{m4}\mathbf{KU}_2 = \bar{\mathbf{R}}_2, \tag{26}$$

with

$$\begin{aligned} \bar{\mathbf{R}}_1 &= \bar{b}_{1m}f_{m1}\mathbf{MU}_0 + \bar{b}_{1m}f_{m2}\mathbf{MV}_0 + \bar{b}_{1m}f_{m3}\mathbf{CU}_0 + \bar{b}_{1m}f_{m4}\mathbf{CV}_0 \\ &\quad + \bar{b}_{1m}f_{m5}\mathbf{KU}_0 + \bar{b}_{1m}f_{m6}\mathbf{KV}_0 + \bar{b}_{11}\mathbf{R}_1 + \bar{b}_{12}\mathbf{R}_2, \\ \bar{\mathbf{R}}_2 &= \bar{b}_{2m}f_{m1}\mathbf{MU}_0 + \bar{b}_{2m}f_{m2}\mathbf{MV}_0 + \bar{b}_{2m}f_{m3}\mathbf{CU}_0 + \bar{b}_{2m}f_{m4}\mathbf{CV}_0 \\ &\quad + \bar{b}_{2m}f_{m5}\mathbf{KU}_0 + \bar{b}_{2m}f_{m6}\mathbf{KV}_0 + \bar{b}_{21}\mathbf{R}_1 + \bar{b}_{22}\mathbf{R}_2. \end{aligned} \tag{27}$$

In Eqs. (25)–(27) the summation over the repeated index m is performed ($m = 1, 2$), and the coefficients $\bar{b}_{ij}$ can be found as elements of the inverse matrix formed by coefficients b_{ij}, see our paper [12]. For example, the explicit expressions of Eqs. (25) and (26) for a particular case with $a \to \infty$ are given as follows:

$$\mathbf{MU}_1 - \frac{\Delta t^2}{6}\mathbf{CU}_2 - \frac{\Delta t^2}{12}\mathbf{KU}_1 - \frac{\Delta t^3}{12}\mathbf{KU}_2 = \mathbf{MV}_0 + \frac{\Delta t}{2}\mathbf{R}_1 - \frac{\Delta t}{2}\mathbf{R}_2 \tag{28}$$

and

$$\mathbf{MU}_2 + \frac{1}{2}\mathbf{CU}_1 + \frac{\Delta t}{2}\mathbf{CU}_2 + \frac{\Delta t}{4}\mathbf{KU}_1 + \frac{\Delta t^2}{6}\mathbf{KU}_2 = -\frac{1}{2}\mathbf{KU}_0 + \frac{1}{2}\mathbf{R}_1, \tag{29}$$

with

$$\mathbf{R}_1 = \frac{1}{\Delta t}\int_0^{\Delta t} \mathbf{R}(t)\,\mathrm{d}t, \quad \mathbf{R}_2 = \frac{1}{\Delta t^2}\int_0^{\Delta t} 2t\mathbf{R}(t)\,\mathrm{d}t. \tag{30}$$

This case corresponds to a non-dissipative numerical scheme.

It is interesting to note that Eqs. (28) and (29) can be written in a matrix form with a symmetric matrix of equations

$$\begin{bmatrix} \left(-\frac{12}{\Delta t^2}\mathbf{M}+\mathbf{K}\right) & (2\mathbf{C}+\Delta t\mathbf{K}) \\ (2\mathbf{C}+\Delta t\mathbf{K}) & \left(4\mathbf{M}+2\Delta t\mathbf{C}+\frac{2\Delta t^2}{3}\mathbf{K}\right) \end{bmatrix} \begin{Bmatrix} \mathbf{U}_1 \\ \mathbf{U}_2 \end{Bmatrix} = \begin{Bmatrix} -\frac{12}{\Delta t^2}\left(\mathbf{M}\mathbf{V}_0+\frac{\Delta t}{2}\mathbf{R}_1-\frac{\Delta t}{2}\mathbf{R}_2\right) \\ -2\mathbf{K}\mathbf{U}_0+2\mathbf{R}_1 \end{Bmatrix}, \tag{31}$$

i.e., a direct sparse solver for symmetric matrices can be used for the implicit method even with a non-proportional physical damping matrix $\mathbf{C}$.

Now the following explicit method with a predictor–multicorrector iterative solver can be suggested for the solutions of Eqs. (25) and (26). We will consider separately two cases without physical damping ($\mathbf{C}=\mathbf{0}$) and with physical damping ($\mathbf{C}\neq\mathbf{0}$).

4.1. The explicit method of the fourth order of accuracy (without physical damping, $\mathbf{C}=\mathbf{0}$)

The following solution procedure for each time step $t_n \leqslant t \leqslant t_{n+1} = t_n + \Delta t$ is proposed:

1. Prescribe initial displacements and velocities:

$$\mathbf{U}_0 = \mathbf{U}(t_n), \quad \mathbf{V}_0 = \mathbf{V}(t_n). \tag{32}$$

2. Calculate the right-hand side vectors $\mathbf{R}_1$ and $\mathbf{R}_2$ at time t_{n+1} according to Eq. (20), and the right-hand side vectors $\bar{\mathbf{R}}_1$ and $\bar{\mathbf{R}}_2$ according to Eq. (27).
3. Predictor:

$$\mathbf{U}_1^0 = \mathbf{V}_0,$$

$$\mathbf{U}_2^0 = \mathbf{M}^{-1}\bar{\mathbf{R}}_2, \tag{33}$$

4. Multicorrector based on Eqs. (25) and (26) ($k = 1, 2, \ldots, l$):

$$\mathbf{U}_1^k = -\bar{b}_{1m}d_{m3}\mathbf{M}^{-1}\mathbf{K}\mathbf{U}_1^{k-1} - \bar{b}_{1m}d_{m4}\mathbf{M}^{-1}\mathbf{K}\mathbf{U}_2^{k-1} + \mathbf{M}^{-1}\bar{\mathbf{R}}_1, \tag{34}$$

$$\mathbf{U}_2^k = -\bar{b}_{2m}d_{m3}\mathbf{M}^{-1}\mathbf{K}\mathbf{U}_1^{k-1} - \bar{b}_{2m}d_{m4}\mathbf{M}^{-1}\mathbf{K}\mathbf{U}_2^{k-1} + \mathbf{M}^{-1}\bar{\mathbf{R}}_2. \tag{35}$$

5. Compute displacements and velocities at time $t_{n+1} = t_n + \Delta t$:

$$\mathbf{U}(t_{n+1}) = \mathbf{U}_0 + \mathbf{U}_1^k\Delta t + \mathbf{U}_2^k\Delta t^2, \quad \mathbf{V}(t_{n+1}) = \mathbf{V}_0 + (2\mathbf{U}_2^k + a_1\mathbf{U}_1^k - a_1\mathbf{V}_0)\Delta t + (a_2\mathbf{U}_1^k - a_2\mathbf{V}_0)\Delta t^2. \tag{36}$$

Here, k is the number of the current iteration ($k = 1, 2, \ldots, l$). The accuracy analysis (see below) shows that only two iterations ($k = 1, 2$) are necessary in order to reach the fourth order of accuracy (the same order of accuracy that a direct solver yields; i.e., when Eqs. (25) and (26) are solved simultaneously). It is necessary to note that for any iteration the corrections of vectors $\mathbf{U}_1^k$ and $\mathbf{U}_2^k$ can be done independently of each other; i.e., they can be paralellized using a parallel computer.

4.2. The explicit method of the fourth order of accuracy (with physical damping, $\mathbf{C}\neq\mathbf{0}$)

The following solution procedure for each time step $t_n\leqslant t\leqslant t_{n+1}=t_n+\Delta t$ is proposed:

1. Prescribe initial displacements and velocities:
$$\mathbf{U}_0=\mathbf{U}(t_n),\quad \mathbf{V}_0=\mathbf{V}(t_n). \tag{37}$$

2. Calculate the right-hand side vectors $\mathbf{R}_1$ and $\mathbf{R}_2$ at time t_{n+1} according to Eq. (20), and the right-hand side vectors $\bar{\mathbf{R}}_1$ and $\bar{\mathbf{R}}_2$ according to Eq. (27).
3. Predictor:
$$\mathbf{U}_1^0=\mathbf{V}_0,\quad \mathbf{U}_2^0=-\bar{b}_{2m}d_{m1}\mathbf{C}\mathbf{U}_1^0-\bar{b}_{2m}d_{m3}\mathbf{M}^{-1}\mathbf{K}\mathbf{U}_1^0+\mathbf{M}^{-1}\bar{\mathbf{R}}_2 \tag{38}$$

4. Multicorrector based on Eqs. (25) and (26) ($k=1,2,\ldots,l$):
$$\begin{aligned}\mathbf{U}_1^k=&-\bar{b}_{1m}d_{m1}\mathbf{M}^{-1}\mathbf{C}\mathbf{U}_1^{k-1}-\bar{b}_{1m}d_{m2}\mathbf{M}^{-1}\mathbf{C}\mathbf{U}_2^{k-1}\\&-\bar{b}_{1m}d_{m3}\mathbf{M}^{-1}\mathbf{K}\mathbf{U}_1^{k-1}-\bar{b}_{1m}d_{m4}\mathbf{M}^{-1}\mathbf{K}\mathbf{U}_2^{k-1}+\mathbf{M}^{-1}\bar{\mathbf{R}}_1,\end{aligned} \tag{39}$$
$$\begin{aligned}\mathbf{U}_2^k=&-\bar{b}_{2m}d_{m1}\mathbf{M}^{-1}\mathbf{C}\mathbf{U}_1^{k}-\bar{b}_{2m}d_{m2}\mathbf{M}^{-1}\mathbf{C}\mathbf{U}_2^{k-1}\\&-\bar{b}_{2m}d_{m3}\mathbf{M}^{-1}\mathbf{K}\mathbf{U}_1^{k}-\bar{b}_{2m}d_{m4}\mathbf{M}^{-1}\mathbf{K}\mathbf{U}_2^{k-1}+\mathbf{M}^{-1}\bar{\mathbf{R}}_2.\end{aligned} \tag{40}$$

5. Additional correction for vector $\mathbf{U}_2$:
$$\begin{aligned}\mathbf{U}_2^{k+1}=&-\bar{b}_{2m}d_{m1}\mathbf{M}^{-1}\mathbf{C}\mathbf{U}_1^{k}-\bar{b}_{2m}d_{m2}\mathbf{M}^{-1}\mathbf{C}\mathbf{U}_2^{k}\\&-\bar{b}_{2m}d_{m3}\mathbf{M}^{-1}\mathbf{K}\mathbf{U}_1^{k}-\bar{b}_{2m}d_{m4}\mathbf{M}^{-1}\mathbf{K}\mathbf{U}_2^{k}+\mathbf{M}^{-1}\bar{\mathbf{R}}_2.\end{aligned} \tag{41}$$

6. Compute displacements and velocities at time $t_{n+1}=t_n+\Delta t$:
$$\begin{aligned}\mathbf{U}(t_{n+1})&=\mathbf{U}_0+\mathbf{U}_1^k\Delta t+\mathbf{U}_2^{k+1}\Delta t^2,\\\mathbf{V}(t_{n+1})&=\mathbf{V}_0+(2\mathbf{U}_2^{k+1}+a_1\mathbf{U}_1^k-a_1\mathbf{V}_0)\Delta t+(a_2\mathbf{U}_1^k-a_2\mathbf{V}_0)\Delta t^2.\end{aligned} \tag{42}$$

Here, k is the number of the current iteration ($k=1,2,\ldots,l$). The accuracy analysis (see below) shows that two iterations ($k=1,2$) are necessary in order to reach the fourth order of accuracy (the same order of accuracy that a direct solver yields; i.e., when Eqs. (25) and (26) are solved simultaneously). In contrast to the case without physical damping, the additional correction of vector $\mathbf{U}_2^k$ is used (see Eq. (41)), and for any iteration the correction of vector $\mathbf{U}_2^k$ depends on the correction of vector $\mathbf{U}_1^k$, see Eqs. (39) and (40). At zero-damping $\mathbf{C}=\mathbf{0}$, the scheme given by Eqs. (37)–(42) can also be used with just one iteration ($k=1$) and without the additional correction for vector $\mathbf{U}_2^k$ (the fourth order of accuracy is achieved). The comparison of this scenario with the numerical scheme given by (32)–(36) is considered below.

4.3. Accuracy analysis

It can be shown (e.g., see Refs. [1,13]) that the analysis of a numerical method for linear dynamics problems Eqs. (1) can be replaced (with the modal decomposition method) by the analysis of the method applied to a system with a single degree of freedom $u(t)$; i.e., the solution of the following simple equations is considered:
$$\dot{v}(t)+2\xi v(t)+\omega^2u(t)=f(t), \tag{43}$$
$$\dot{u}(t)-v(t)=0, \tag{44}$$

where ω and f are the natural frequency and forcing excitation, respectively, $v(t)$ is the velocity, ξ is the damping ratio. For the analysis of the accuracy and stability of the numerical methods, the interval J_n from 0 to Δt is considered.

The values of u_n and v_n at time $t=t_n$ can be expressed in terms of initial values u_0 and v_0 in the beginning of the interval J_n as

$$\begin{Bmatrix} u_n \\ v_n \end{Bmatrix} = [A] \begin{Bmatrix} u_0 \\ v_0 \end{Bmatrix} + [L]f, \tag{45}$$

where $[A]$ is the amplification matrix, and $[L]$ is the load matrix. Without loss of generality we can assume that $t_{n-1}=0$ and $t_n - t_{n-1} = \Delta t$.

The analytical expression of matrix $[A]$ in Eq. (45) for direct and predictor/multi-corrector solvers can be calculated from the application of the corresponding method to the system with a single degree of freedom, Eqs. (43), (44), at the condition $f(t)=0$. The analytical expressions of the expansion of the elements of the exact matrix $[A]$ into the Taylor series can be found in our papers [12,13].

The accuracy of the new TCG method can be estimated by the application of this method to system (43), (44) and by the comparison of the numerical and exact amplification matrices (see Refs. [1,13]).

The stability of an algorithm can be observed from the spectral radius defined by $r(\mathbf{A}) = \max|\rho_1, \rho_2|$, where ρ_1 and ρ_2 denote the eigenvalues of the amplification matrix $[A]$ (see Ref. [1]). An algorithm that satisfies the condition $r([A]) \leqslant 1$ is said to be unconditionally stable. It is known that the higher modes of semidiscrete structural equations do not represent the behavior of the governing partial differential equations. Therefore, algorithmic damping (dissipation) is necessary in order to remove the participation of the high-frequency modal components. The numerical dissipation of the algorithm over the entire frequency domain can be observed from the spectral radius. The condition $r([A])=1$ for some frequencies corresponds to non-dissipative behavior, and $r([A])<1$ for some frequencies corresponds to the introduction of the numerical dissipation. It is desirable to design a numerical algorithm with non-dissipative properties at low frequencies and with large numerical dissipation at high frequencies.

First, let us analyze the new explicit method for the case without physical damping. For the numerical scheme with two iterations (see Eqs. (32)–(36)), the elements of the matrix $[A]$ depend on the scalar parameter a and are given in Appendix A. The variation of parameter a does not affect the order of accuracy, but changes the numerical dissipation (the minimum spectral radius) and the stability limit of the method. E.g., the highest-order terms in the expansion of the elements of the matrix $[A]$ into the Taylor series, which differ from those of the exact matrix $[A]$, are given below for the case $a=\infty$:

$$A_{11} = A_{22} = O[\Delta t]^6, \quad A_{12} = -A_{21}/\omega^2 = \cdots + \frac{\omega^4 \Delta t^5}{144} + O[\Delta t]^6, \tag{46}$$

i.e., the method has the fourth order of accuracy. The corresponding spectral radius, algorithmic damping ratios and relative period errors for $a=\infty$ are shown in Figs. 1a, b and 2 (where $\Omega = \omega \Delta t$). The stability limit is $\Omega^s = 3.46$ at $a=\infty$. There is no bifurcation of eigenvalues before the stability limit for $\Omega \leqslant \Omega^s$. The minimum value of the spectral radius is $r_{\min} = 0.13$ at $\Omega^m = 3.1$. For $a = \Delta t/0.204$ (the parameter a is responsible for the value of numerical dissipation), the minimum value of the spectral radius $r_{\min}$ is close to zero at $\Omega = \Omega^m = 3.051$ (see Fig. 1b). $\Omega = \Omega^m = 3.051$ is also the bifurcation point. At the variation of the parameter a between $\Delta t/0.204 < a < \infty$, the spectral radius changes gradually between two curves shown in Fig. 1b. At $a < \Delta t/0.204$, the minimum spectral radius increases, the stability limit decreases and the spectral radius at small frequencies decreases; i.e., this range for the parameter a should not be used in calculations. It is necessary to note that the explicit TDG method developed in Ref. [6] and called 'E-2C' requires the same computational efforts as the new explicit method with two iterations. However, the explicit TDG method has the third order of accuracy, a stability limit of only $\Omega^s = 2.223$, and yields greater error at small frequencies (see Figs. 1a and 2). For comparison, the spectral radii of the two popular second-order explicit methods, the central difference method (no numerical dissipation) and the HCE-α method (with numerical dissipation) [2], are shown in Fig. 1a (the minimum spectral radii for the HCE-α and 'E-2C' methods were selected to be $r_{\min} = 0.6$).

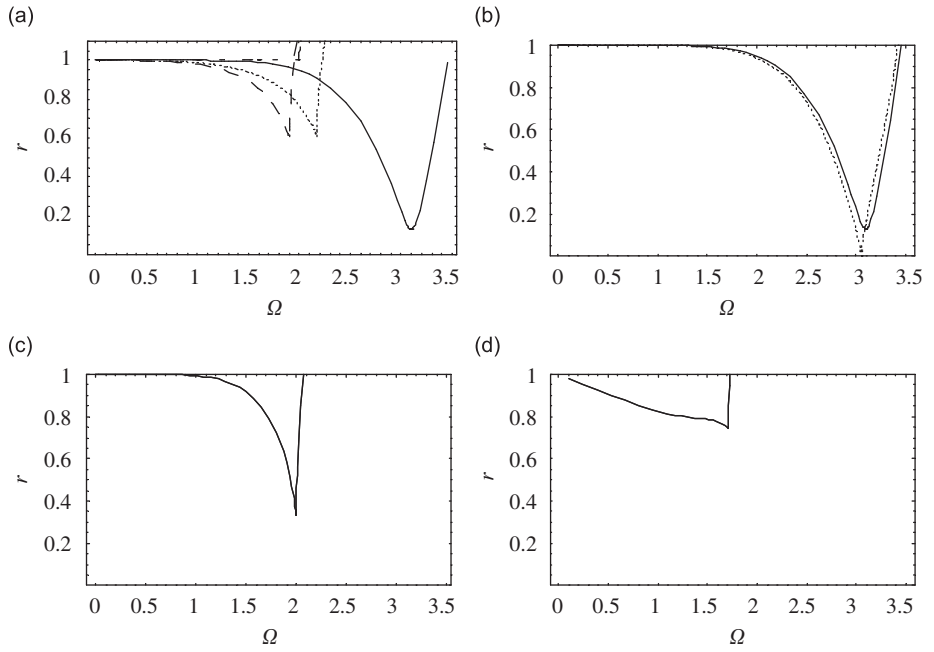

Fig. 1. Spectral radii r of the numerical amplification matrix [A]. (a) (—) corresponds to the new explicit TCG method with two passes and zero-damping matrix $\mathbf{C}=\mathbf{0}$ ($a=\infty$); (· · · ·) corresponds to the explicit TDG method ('E-2C') proposed in Ref. [6]; (- - -) corresponds to the explicit HCE-α method proposed in Ref. [2]; (- · - · -) corresponds to the explicit central difference method; (b) corresponds to the new explicit TCG method with two passes and zero-damping matrix $\mathbf{C}=\mathbf{0}$ ((—) corresponds to $a=\infty$, (· · · ·) corresponds to $a=\Delta t/0.204$); (c) corresponds to the new explicit TCG method with one pass, no additional correction for vector $\mathbf{U}_2^k$ and zero-damping matrix $\mathbf{C}=\mathbf{0}$ ($a=\infty$); (d) corresponds to the new explicit TCG method with two passes and non-zero physical damping $\xi=0.2$ ($a=\infty$).

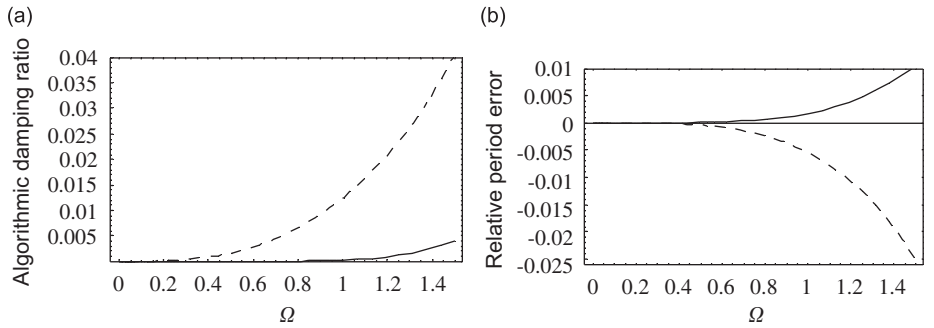

Fig. 2. Algorithmic damping ratios (a), and relative period errors (b), for the new explicit TCG method with $a=\infty$ (—) and the explicit TDG method ((- - -), see Ref. [6]) with two passes and zero-damping matrix $\mathbf{C}=\mathbf{0}$.

Remark. The implicit TCG method with $a=\infty$ has no numerical dissipation, however, the explicit TCG method with $a=\infty$, derived from the implicit TCG method, has numerical dissipation, see Fig. 1a,b.

For the numerical scheme given by Eqs. (37)–(42) with one iteration and no additional correction for the vector U_2^k, the method has also the fourth order of accuracy. For $a=\infty$ the spectral radius of the numerical amplification matrix [A] is shown in Fig. 1c. The bifurcation point and stability limit are close to $\Omega^s=2$. The minimum value of the spectral radius is $r_{\min}=1/3$ at $\Omega=\Omega^m=2$, see Fig. 1c. The explicit TDG method developed in Ref. [6] and called 'E-1C' requires the same computational efforts as the new explicit method given by Eqs. (37)–(42) with one iteration, but has the third order of accuracy only.

For the explicit method given by Eqs. (37)–(42) with two iterations ($\mathbf{C}\neq\mathbf{0}$), the highest-order terms in the expansion of the elements of the matrix $[A]$ into the Taylor series, which differ from those of the exact

matrix [A], are given below for the case $a=\infty$:

$$A_{11}=A_{22}=\cdots+\frac{\omega^6\Delta t^6}{96}+O[\Delta t]^7,\quad A_{12}=O[\Delta t]^5,\quad A_{21}=\cdots+\frac{\omega^6\Delta t^5}{48}+O[\Delta t]^6, \tag{47}$$

i.e., the method has the fourth order of accuracy. For $a=\infty$ and $\xi=0.2$, the spectral radius of the numerical amplification matrix [A] is shown in Fig. 1d. The stability limit decreases with the increase in physical damping (the parameter ξ). For example, at $\xi=0.2$ the stability limit is $\Omega^s=1.7$, see Fig. 1d.

5. Numerical examples

The new technique is implemented into the finite-element code FEAP [3]. Simple numerical tests show that the numerical stability limit for the new explicit method is in good agreement with the theoretical results. Next, we will consider two numerical examples in order to show the performance of the new method.

5.1. Undamped single degree of freedom

Let us consider free vibrations of a simple undamped oscillator described by Eqs. (43) and (44) with a natural frequency equal to $\omega=2\pi$, zero-damping $\xi=0$, zero forcing excitation $f(t)=0$ and the following initial conditions: $u(0)=1$ and $v(0)=0$. The analytical solution for this problem is $u_a(t)=\cos(2\pi t)$ and $v_a(t)=-2\pi\sin(2\pi t)$. The problem was solved with the new explicit method with two passes given by Eqs. (32)–(36) and with the new explicit method with one pass given by Eqs. (37)–(42) ($\mathbf{C}=\mathbf{0}$) using different time increments Δt (the parameter $a=\infty$ was taken). The numerical error in displacements and velocities was calculated as

$$e=\sqrt{(u_n(T)-u_a(T))^2+(v_n(T)-v_a(T))^2}, \tag{48}$$

where u_n and v_n correspond to a numerical solution for displacements and velocities, and the observation time T is chosen to be $T=4$. The numerical error against a time increment Δt in a double logarithmic scale is shown in Fig. 3. As expected, both the new explicit methods have the fourth order of accuracy (the slopes of curves in Fig. 3 provide the order of accuracy). As can be seen from Fig. 3, at the same accuracy the method with two passes given by Eqs. (32)–(36) requires approximately half the time increments that the method with one pass given by Eqs. (37)–(42) requires; i.e., the computational costs of both methods are approximately the same. However, the method with two passes has a much larger stability limit $\Omega^s=3.46$ ($\Omega^s=2$ for the method with one pass). For comparison, the problem was also solved by the central difference method. It can be seen from Fig. 3, that the fourth-order method is much more effective if the accuracy is a critical issue (e.g., due to the accumulation of the numerical error at long-term time integration).

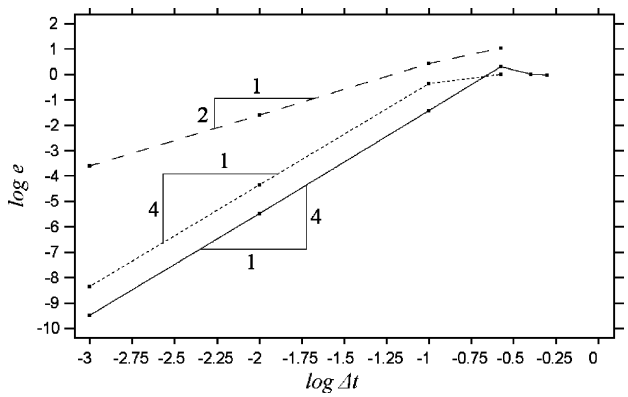

Fig. 3. Numerical error $\log e$ against a time increment $\log\Delta t$ for free vibrations of a simple undamped oscillator ($T=4$). (—) corresponds to the method with two passes given by Eqs. (32)–(36), (· · · ·) corresponds to the method with one pass given by Eqs. (37)–(42), and (- - -) corresponds to the central difference method.

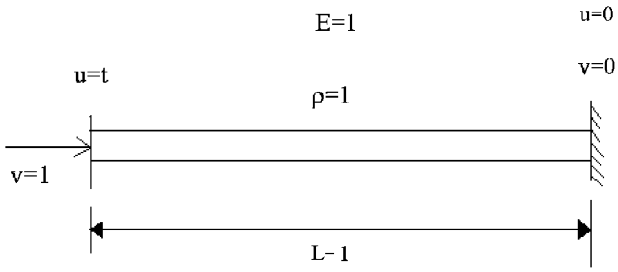

Fig. 4. Impact of an elastic bar against a rigid wall.

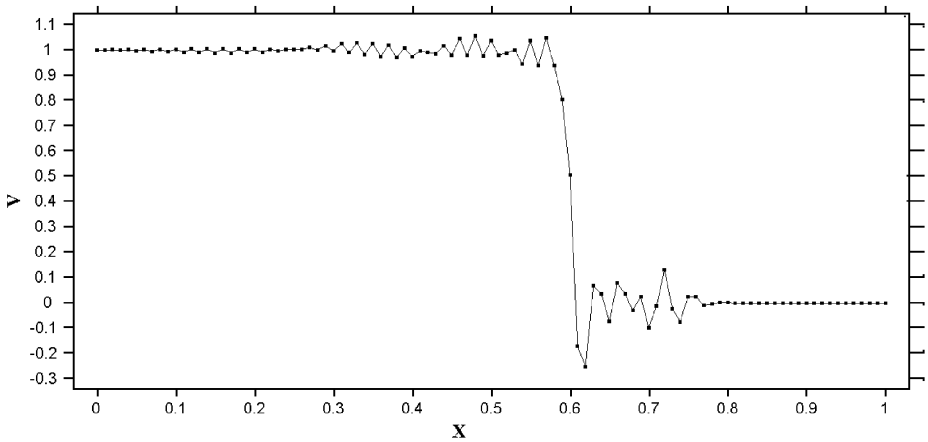

Fig. 5. Velocity distribution along the bar at time $T = 0.6$ computed on the uniform mesh containing 100 quadratic elements using the standard central difference method with 150 time increments ($\Delta t = 0.004$).

5.2. Impact of an elastic bar against a rigid wall

Impact against a rigid wall of an elastic rod of the length $L = 1$ (see Fig. 4) is considered. The right end of the rod is fixed ($u(1,t) = v(1,t) = 0$), the velocity $v = 1$ is instantly applied at the left end ($u(0,t) = t, v(0,t) = 1$), and the initial displacements and velocities are zero. Zero-damping is assumed ($\mathbf{C} = \mathbf{0}$). The observation time T is chosen to be $T = 0.6$; the Young's modulus is $E = 1$, and the density is $\rho = 1$. The problem was solved with 100 quadratic 3-node finite elements. The highest frequency for the mesh considered is $w_{\max} = 500$. This value is important for the selection of the maximum time increment that satisfies the stability criterion. The problem has the continuous solution for displacements $u_a(x,t) = t - x$ for $t \geqslant x$ and $u_a(x,t) = 0$ for $t \leqslant x$, and the discontinuous solution for velocities and stresses $v_a(x,t) = -\sigma^a(x,t) = 1$ for $t \geqslant x$ and $v_a(x,t) = \sigma^a(x,t) = 0$ for $t \leqslant x$ (at the interface $x = t$ jumps in stresses and velocities occur).

It is known that the application of the traditional semi-discrete methods to this problem leads to oscillations in velocities and stresses due to the spurious high-frequency response (see Refs. [14,15]). The standard implicit TDG method also yields spurious oscillations for this problem, especially on non-uniform meshes in space (see Refs. [12,13]). Numerical methods with controllable numerical dissipation at high frequencies are necessary in order to suppress these oscillations. High-order accurate implicit methods with these properties that correctly solve the problem under consideration are developed in Refs. [12,13]. Here we will consider the application of the new explicit high-order accurate method to this problem. For comparison, the solution of the problem with the classical central difference method (150 time increments $\Delta t = 0.004$) is shown in Fig. 5. Due to the absence of numerical dissipation, the solution in Fig. 5 contains spurious oscillations that do not disappear with the decrease in time increments (except the case when linear elements in space are used, and the time increment equals the characteristic time step, see Ref. [1]). The solution obtained by the new explicit

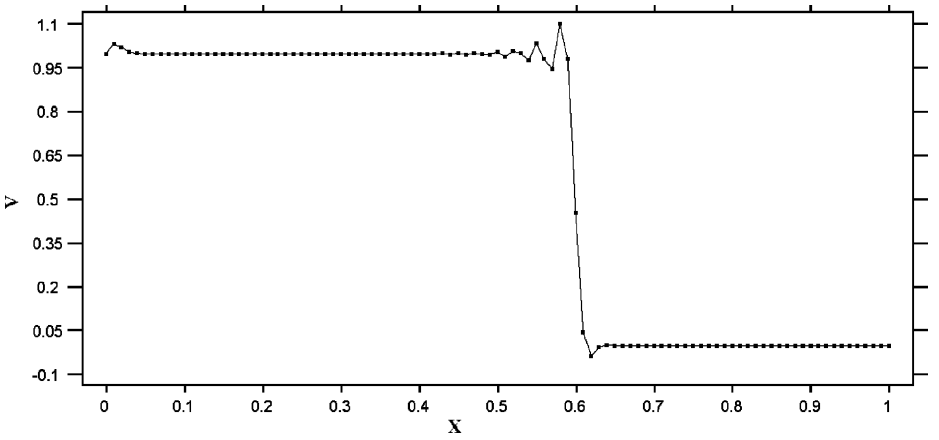

Fig. 6. Velocity distribution along the bar at time $T = 0.6$ computed on the uniform mesh containing 100 quadratic elements using the new explicit TCG method with 100 time increments ($\Delta t = 0.006$).

method (100 time increments $\Delta t = 0.006$ and $a = 0.006/0.204$) is much better (see Fig. 6), however, few oscillations remain. To improve this solution we are going to develop a new solution strategy for explicit methods (using the ideas described in our paper Ref. [12] for implicit methods).

6. Concluding remarks

A new explicit predictor–multicorrector fourth-order accurate method for linear elastodynamics is suggested in the paper. In contrast to recently suggested explicit third-order accurate methods based on the TCG method, the new method is more accurate (has a higher-order of accuracy) and has better algorithmic properties (e.g., a higher-stability limit) at the same computational efforts. The method has controllable numerical dissipation with zero spectral radius at some values of the variable Ω, however it cannot completely suppress all high-frequency oscillations for wave propagation problems (similar to other known explicit methods). In the future, we are going to develop a new solution strategy for explicit methods (using the ideas described in our paper Ref. [12] for the solution strategy with implicit methods) in order to suppress all high-frequency oscillations retaining high accuracy of numerical results. The extension of the new fourth-order accurate method to nonlinear problems can be made similarly to the approach suggested in Ref. [16], and will be considered elsewhere. As a possible application of the new technique, we will consider wave propagation problems in composite materials with average elastic properties, see Ref. [17].

Acknowledgments

AVI gratefully acknowledges the support of the Texas Higher Education Coordinating Board under Grant 003644 0008 2006, as well as the support of the Air Force Summer Faculty Fellowship Program 2006 and Texas Tech University.

Appendix A

Elements of the numerical amplification matrix $[A]$ for the new fourth-order accurate explicit method with two iterations (see Eqs. (32)–(36)) are given below (where $c = \Delta t/a$)

$$A_{11} = \frac{1}{20000(c^2+6c+12)^4}[(207w^6\Delta t^6 + 300w^4\Delta t^4 - 10000w^2\Delta t^2 + 20000)c^8 + 12(321w^6\Delta t^6 + 850w^4\Delta t^4 - 20000w^2\Delta t^2 + 40000)c^7 + 12(2687w^6\Delta t^6 + 11600w^4\Delta t^4 - 220000w^2\Delta t^2 + 440000)c^6$$

$$+128(1212w^6\Delta t^6+8275w^4\Delta t^4-135000w^2\Delta t^2+270000)c^5$$
$$+80(5741w^6\Delta t^6+62820w^4\Delta t^4-918000w^2\Delta t^2+1836000)c^4$$
$$+160(5171w^6\Delta t^6+96240w^4\Delta t^4-1296000w^2\Delta t^2+2592000)c^3$$
$$+19200(43w^6\Delta t^6+1560w^4\Delta t^4-19800w^2\Delta t^2+39600)c^2$$
$$+48000(7w^6\Delta t^6+708w^4\Delta t^4-8640w^2\Delta t^2+17280)c$$
$$+17280000(w^4\Delta t^4-12w^2\Delta t^2+24)] \quad (A.1)$$

$$A_{12}=-A_{21}/\omega^2=\frac{1}{2000(c^2+6c+12)^3}\{w^2\Delta t[(27w^4\Delta t^4+300w^2\Delta t^2-2000)c^6$$
$$+(258w^4\Delta t^4+5600w^2\Delta t^2-36000)c^5+4(177w^4\Delta t^4+11500w^2\Delta t^2-72000)c^4$$
$$-1600(w^4\Delta t^4-132w^2\Delta t^2+810)c^3-480(29w^4\Delta t^4-1190w^2\Delta t^2+7200)c^2$$
$$-2400(13w^4\Delta t^4-360w^2\Delta t^2+2160)c-24000(w^2\Delta t^2-12)^2]\} \quad (A.2)$$

$$A_{22}=\frac{1}{200(c^2+6c+12)^2}[(3w^4\Delta t^4-100w^2\Delta t^2+200)c^4$$
$$+6(11w^4\Delta t^4-200w^2\Delta t^2+400)c^3+60(7w^4\Delta t^4-100w^2\Delta t^2+200)c^2$$
$$+40(29w^4\Delta t^4-360w^2\Delta t^2+720)c+1200(w^4\Delta t^4-12w^2\Delta t^2+24)]. \quad (A.3)$$

References

[1] T.J.R. Hughes, *The Finite Element Method: Linear Static and Dynamic Finite Element Analysis*, Prentice-Hall, Englewood Cliffs, NJ, 1987.
[2] G.M. Hulbert, J. Chung, Explicit time integration algorithms for structural dynamics with optimal numerical dissipation, *Computer Methods in Applied Mechanics and Engineering* 137 (2) (1996) 175–188.
[3] O.C. Zienkiewicz, R.L. Taylor, *The Finite Element Method*, Butterworth-Heinemann, Oxford, UK, 2000.
[4] M.G. Katona, O.C. Zienkiewicz, Unified set of single step algorithms—part 3: the beta-m method, a generalization of the newmark scheme, *International Journal for Numerical Methods in Engineering* 21 (7) (1985) 1345–1359.
[5] O.C. Zienkiewicz, W.L. Wood, N.W. Hines, R.L. Taylor, Unified set of single step algorithms—part i: general formulation and applications, *International Journal for Numerical Methods in Engineering* 20 (8) (1984) 1529–1552.
[6] A. Bonelli, O.S. Bursi, Explicit predictor–multicorrector time discontinuous Galerkin methods for linear dynamics, *Journal of Sound and Vibration* 246 (4) (2001) 625–652.
[7] T.C. Fung, Construction of higher-order accurate time-step integration algorithms by equal-order polynomial projection, *Journal of Vibration and Control* 11 (1) (2005) 19–49.
[8] C. Hoff, R.L. Taylor, Higher derivative explicit one step methods for non-linear dynamic problems. part i: design and theory, *International Journal for Numerical Methods in Engineering* 29 (2) (1990) 275–290.
[9] T.J.R. Hughes, G.M. Hulbert, Space–time finite element methods for elastodynamics: formulations and error estimates, *Computer Methods in Applied Mechanics and Engineering* 66 (3) (1988) 339–363.
[10] M. Mancuso, F. Ubertini, A methodology for the generation of low-cost higher-order methods for linear dynamics, *International Journal for Numerical Methods in Engineering* 56 (13) (2003) 1883–1912.
[11] N.E. Wiberg, X.D. Li, Adaptive finite element procedures for linear and non-linear dynamics, *International Journal for Numerical Methods in Engineering* 46 (10) (1999) 1781–1802.
[12] A.V. Idesman, A new high-order accurate continuous Galerkin method for linear elastodynamics problems, *Computational Mechanics* 40 (2) (2007) 261–279.
[13] A.V. Idesman, Solution of linear elastodynamics problems with space-time finite elements on structured and unstructured meshes, *Computer Methods in Applied Mechanics and Engineering* 196 (2007) 1787–1815.
[14] G.M. Hulbert, Discontinuity-capturing operators for elastodynamics, *Computer Methods in Applied Mechanics and Engineering* 96 (3) (1992) 409–426.
[15] G.M. Hulbert, T.J.R. Hughes, Space-time finite element methods for second-order hyperbolic equations, *Computer Methods in Applied Mechanics and Engineering* 84 (3) (1990) 327–348.
[16] A. Bonelli, O.S. Bursi, M. Mancuso, Explicit predictor–multicorrector time discontinuous Galerkin methods for non-linear dynamics, *Journal of Sound and Vibration* 256 (4) (2002) 695–724.
[17] R.L. Sierakowski, S.K. Chaturvedi, *Dynamic Loading and Characterization of Fiber-Reinforced Composites*, Wiley, New York, 1997.